horticulturae

MDPI

Article

Multispectral Imaging Enables High-Throughput Detection of Feijoa Fruit Defects

Anastasia Zolotukhina [1], Svetlana Batashova [1], Anastasia Guryleva [1,*], Natalia Platonova [2], Victoria Kunina [2] and Alexander Machikhin [1]

[1] Acousto-Optic Spectroscopy Lab, Scientific and Technological Centre of Unique Instrumentation, Russian Academy of Sciences, Moscow 117342, Russia; zolotukhina.aa@ntcup.ru (A.Z.); machikhin@ntcup.ru (A.M.)
[2] Federal Research Centre the Subtropical Scientific Centre of the Russian Academy of Sciences, Sochi 354002, Russia
* Correspondence: guryleva.av@ntcup.ru

Abstract

Feijoa fruits are known for their pronounced post-harvest ripening. Phytopathogen-infected specimens pose a significant risk to storage stability and overall fruit quality. Early detection and removal of defective fruits during the initial storage stages are critical for maintaining market value and preventing the spread of disease. In this study, we analyze how the multispectral reflectance properties of the feijoa surface change in response to various defects. 'Superba' cultivar fruits were selected, including healthy controls and samples exhibiting bruises, anthracnose, stink bug damage, tissue suberization, and gray mold. Biochemical analyses were conducted to measure the levels of organic acids, sugars, ascorbic acid, and total polyphenols. Multispectral imaging was performed with a 12-channel camera operating in the 400–1000 nm wavelength range. Results showed that the fruits affected by gray mold had the lowest concentrations of malic and citric acids but the highest levels of succinic acid. Fruits with anthracnose or insect damage exhibited the highest sugar content. Distinct differences in spectral reflectance were observed between healthy and affected areas of fruit. Based on these findings, an image processing algorithm for defective fruit detection was developed.

Keywords: feijoa; storage; biochemical indicators; multispectral imaging; spectral reflectance; defect detection

1. Introduction

Feijoa sellowiana 'Superba' is a promising Californian cultivar of the Myrtaceae family, currently dominant in Russia's humid subtropical regions. This cultivar holds significant economic potential as a monodominant taxon due to its resilience to both abiotic and biotic stressors, broad ecological adaptability, and high yield. Although feijoa fruits are generally resistant to pathogens and pests common in humid subtropical climates, several phytopathological abnormalities are often observed during post-harvest ripening. These include localized subcutaneous necrosis (bruising), anthracnose, insect damage, tissue suberization (corking), and gray mold development. [1–3].

Like other fruits with noticeable post-harvest ripening, feijoa exhibits two stages of maturity: the technical (harvest) stage, which ensures transport resilience, and the consumer stage, reached after 7–15 days of storage. During this period, the mesocarp softens, volatile aromatic compounds are produced, and the epidermal color changes from emerald green to yellowish green. Fruits affected by phytopathologies in a batch pose

Check for updates

Academic Editors: Xiaoli Tan and Yingying Yang

Received: 3 March 2026
Revised: 9 April 2026
Accepted: 14 April 2026
Published: 16 April 2026

Copyright: © 2026 by the authors. Licensee MDPI, Basel, Switzerland. This article is an open access article distributed under the terms and conditions of the Creative Commons Attribution (CC BY) license.

risks at both maturity stages. At the technical stage, subcutaneous necrosis and tissue suberization can damage texture and reduce storage stability, leading to increased transport losses [4]. Anthracnose and gray mold can spread rapidly in humid conditions, posing a serious threat during long-distance logistics. Damage caused by the brown marmorated stink bug weakens the peel, making it easier for secondary pathogens to invade [5]. At the consumer stage, such fruits lose their organoleptic qualities: the pulp may become watery or overly firm, and bitter or sour flavors may develop, reducing product appeal. Fungal infections can compromise the quality of the entire batch, shorten shelf life, and cause significant economic losses [6].

Early removal of defective fruits is crucial for ensuring high product quality and preventing the spread of disease. Visual inspection of fresh feijoa fruits must be performed to evaluate external appearance and assign the appropriate commercial grade. However, visual evaluation is subjective, less effective for detecting hidden defects, labor-intensive, and inefficient for high-throughput screening [7]. Destructive quality control methods [8], such as biochemical and respiration rate analyses, provide detailed insight into physiological changes, but are unsuitable for large-scale monitoring [9]. There are promising non-destructive methods for detecting fruit damage, including imaging spectroscopy, optical coherence tomography, fluorimetry, nuclear magnetic resonance spectroscopy, thermography, and acoustic techniques [10–12]. Among them, imaging spectroscopy [13], including multispectral imaging, is one of the most effective as it enables simultaneous analysis of surface defects and internal tissue structure through spatial mapping of spectral characteristics [14]. To develop a detection algorithm for feijoa fruits and enable classification using spectral images, it is necessary to study the multispectral reflectance of healthy fruits and those affected by common phytopathologies. This study aims to investigate the patterns of reflectance changes on the surface of feijoa fruits affected by phytopathogens using a multispectral camera.

2. Materials and Methods

2.1. Experimental Samples

For this study, we selected *Feijoa sellowiana* fruits of the 'Superba' cultivar, grown at the experimental orchards of the Subtropical Scientific Centre of the Russian Academy of Sciences. The fruits were uniformly selected for quality at a consumer stage of ripeness in dry, warm weather. From this batch, we selected samples from 30 biological replicates, including healthy fruits (control) and fruits exhibiting the following common phytopathological symptoms.

(1) Bruising (localized subcutaneous necrosis): Fruits damaged by impact (e.g., dropping to the ground) develop micro-injuries that serve as entry points for pathogens. This effect initiates biochemical degradation by activating enzymes such as polyphenol oxidase, which causes pulp browning. Increased respiration accelerates metabolism and nutrient depletion, reducing shelf life. If not promptly removed, such fruits can raise the risk of infection across the batch and reduce commercial quality.

(2) Anthracnose: Caused by the ascomycete *Colletotrichum gloeosporioides* (order Glomerellales), this disease leads to necrotic lesions on the fruit skin, significantly lowering market quality. It spreads through contact with damaged tissue (scratches, cracks), contaminated packaging and equipment (where spores can survive up to three months), or leaking infected sap, which supports secondary microbial growth. An infected fruit can contaminate surrounding ones, especially under high humidity.

(3) Damage by Brown marmorated stink bug *Halyomorpha halys*: This pest feeds by piercing the fruit's skin and extracting sap, disrupting vascular tissues and stunting fruit

development. The resulting necrotic lesions (1–3 mm) foster pathogen penetration. Infestation can lead to significant yield loss in heavily affected orchards.

(4) Suberization (cork formation): As a natural protective response to mechanical injuries or abiotic stress (e.g., hail or humidity fluctuations), suberin and waxes spread in the damaged area. While these protect the tissue, they also cause surface scarring, thereby reducing the fruit's visual appeal and marketability.

(5) Early-stage gray mold Botrytis cinerea: This highly infectious pathogen spreads rapidly in humid conditions and through even minor skin damage. While initial contamination may be limited, gray mold can nearly spoil a batch if left unchecked. Additionally, the fungus produces ethylene and other metabolites that speed up ripening and aging in surrounding fruits, increasing their vulnerability to further spoilage.

2.2. Experimental Equipment

For multispectral imaging, we used a custom-designed, scanning-free camera [15] equipped with evenly spaced spectral channels covering the 400–1000 nm range, each with a 10 nm bandwidth at half-maximum (Figure 1a). Uniform illumination was achieved using two 150 W halogen light sources (Dedolight DLH4, Dedo Weigert Film, München, Germany). Samples were placed inside a polycarbonate light diffuser. Images were captured at an exposure time of 500 µs from both sides. Six fruit categories were imaged in thirty biological replicates each (Figure 1b–g). A calibration target with uniform reflectance across the spectrum was used for radiometric correction under identical imaging conditions.

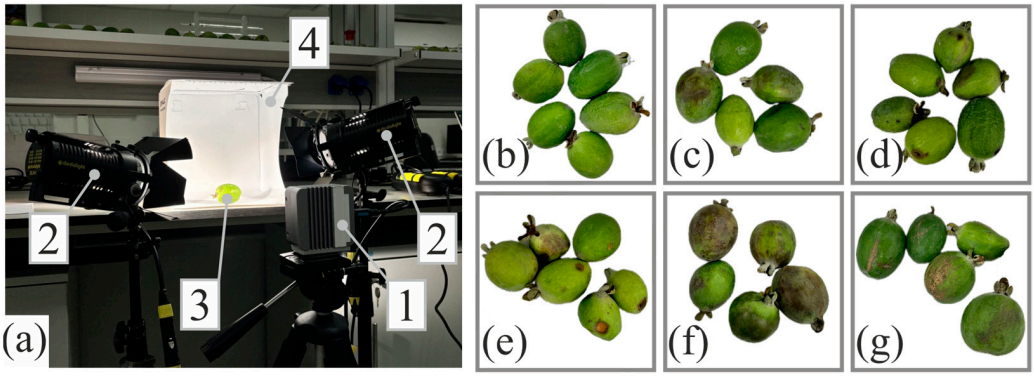


Figure 1. Image acquisition setup (**a**): 1—multispectral camera, 2—light sources, 3—sample, 4—light diffuser; fruit samples: healthy (**b**), bruised (**c**), anthracnose-infected (**d**), damaged by stink bug (**e**), with a gray mold (**f**), and with a suberized skin (**g**).

A biochemical analysis was conducted to assess changes in quality between infected and healthy fruits. Levels of organic acids, carbohydrates, and ascorbic acid were measured using the Kapel-105M capillary electrophoresis system («Lumex», Saint Petersburg, Russia) with a quartz capillary (75 µm ID, 0.6 m effective length), liquid thermosetting, and microcentrifuge IKA mini G («IKA Werke», Staufen, Germany) at 13,000 rpm. Data were processed with the Elforan software package (5.1.0 version). Total polyphenol content was determined with a UNICO 2800 (UNICO, Franksville, WI, USA), a single-beam scanning spectrophotometer with Folin–Ciocalteu reagent.

2.3. Data Processing

The main stages of the processing algorithm are presented in Figure 2. To minimize the influence of imaging artifacts such as uneven lighting, detector sensitivity, optical aberrations, and nonlinearity, spatio-spectral calibration was performed using an integrating sphere (LabSphere FT-2200-W, «Labsphere», North Sutton, NH, USA), a checkerboard

target, and diffuse reflectance standards. After image correction, radiometric calibration was applied by dividing the sample images by the reference panel image [16]. Reflectance spectra were obtained by averaging pixel values over manually selected regions of interest based on color images of the fruit. The final reflectance values were reported as mean, maximum, and minimum across replicates for each spectral band.

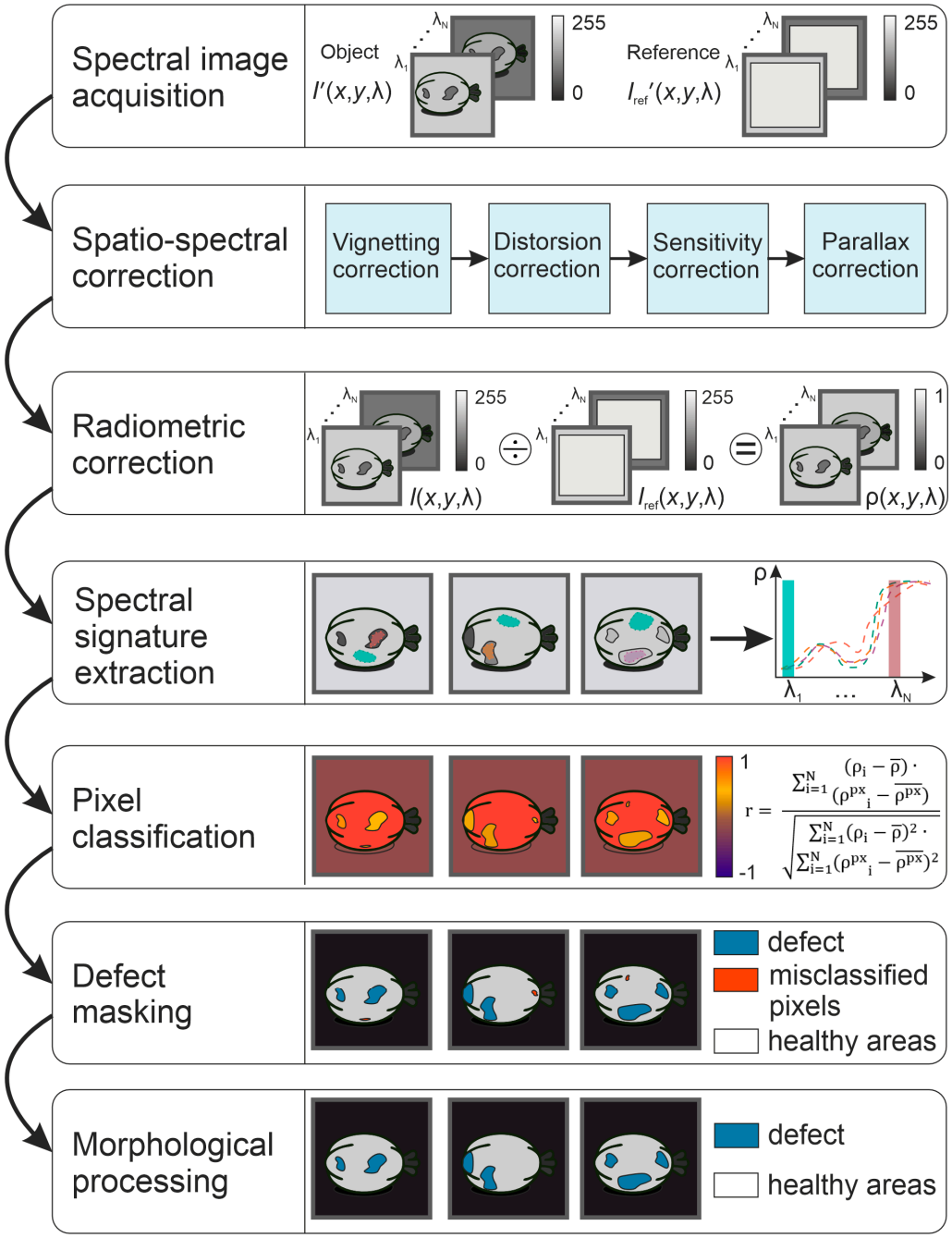


Figure 2. Image processing pipeline for spectral defect detection.

The defect detection process in spectral images involved several key stages. First, regions of interest were manually selected to extract spectral signatures from both healthy and affected areas (Figure 3). The current standard for routine fruit quality assessment is visual inspection of the fruit peel. However, this method lacks objectivity and efficiency; therefore, multispectral imaging could serve as a valuable alternative. We present our results as an objective, automated, and reliable method to replace visual inspection. Ac-

cordingly, annotations from this analysis were used as the reference. Two experts in fruit storage independently generated the reference annotations. In cases of discrepancies in the experts' coordinate assessments, the values were averaged. For all data, differences did not exceed 5%. The criteria for classifying a region as defective included changes in peel color and texture, as well as defect-specific morphological features.

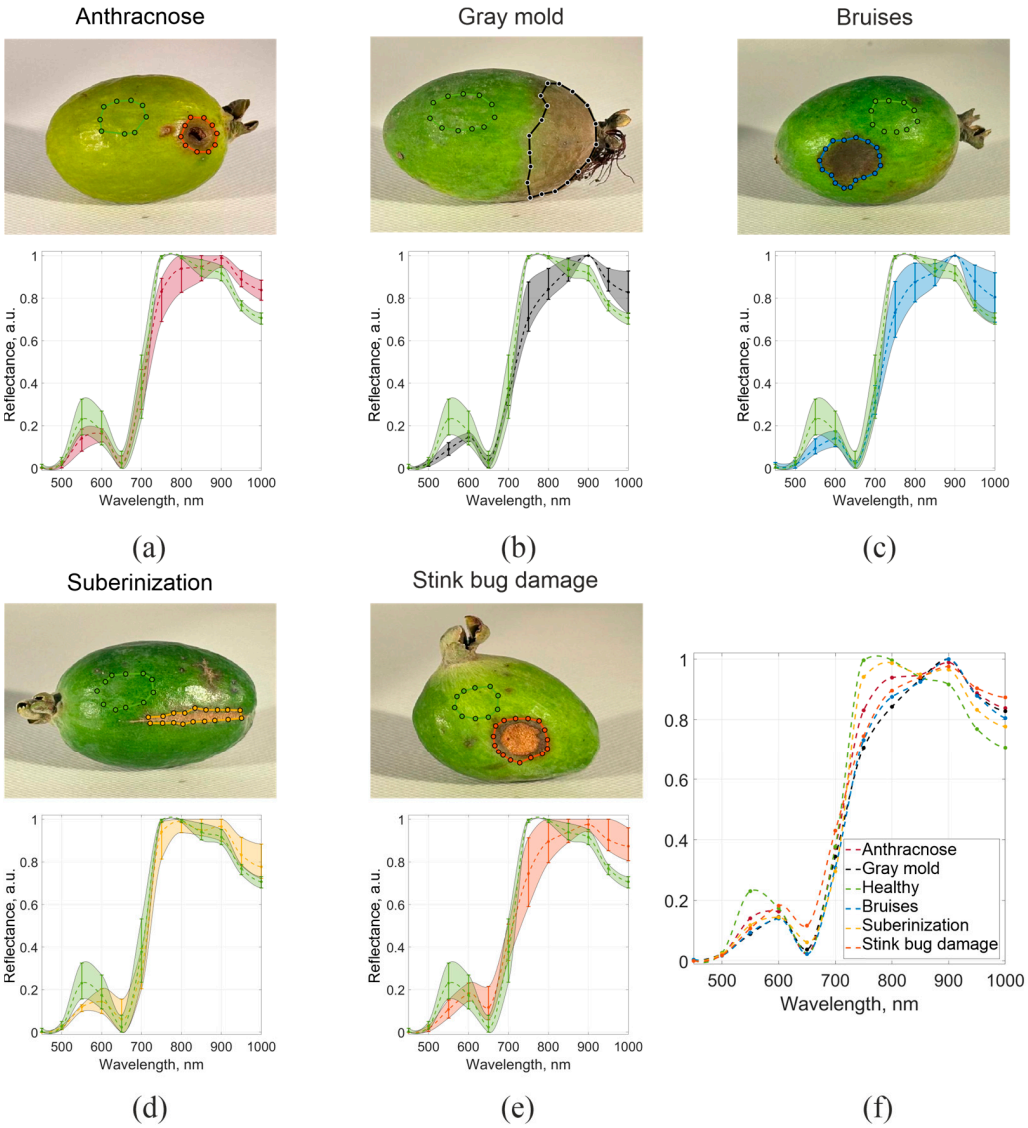


Figure 3. Spectral reflectance of healthy and damaged fruit areas. Individual defect types (**a**–**e**): images showing the damage area at the top and spectral reflectance of healthy and damaged fruit areas at the bottom. The plots display the average and scatter values of spectral reflectance for healthy (green) and damaged areas (anthracnose—scarlet, gray mold—black, bruises—blue, suberinization—yellow, stink bug damage—red). The average value is shown by a dashed line, and the spread is the filled area. The average spectral reflectance plots for all defect types are shown in (**f**).

Figure 3 shows the spectral reflectance coefficients of feijoa fruits with different types of damage, along with the variability within each group across the multispectral camera's spectral channels. The spectral curves indicate that healthy fruit areas differ markedly from diseased ones, especially at 550 nm, 750 nm, 950 nm, and 1000 nm wavelengths. The reflectance from areas affected by anthracnose exhibits a noticeable deviation in the channel centered at 650 nm (Table 1).

Table 1. Average and scatter values of spectral reflectance of healthy and different defect types.

Central Wavelength, nm	Spectral Reflectance of Different Defect Types					
	Healthy	Anthracnose	Gray Mold	Bruises	Suberinization	Stink Bug Damage
450	0.01 ± 0.01	0.00 ± 0.00	0.00 ± 0.00	0.01 ± 0.01	0.00 ± 0.00	0.00 ± 0.00
500	0.03 ± 0.02	0.02 ± 0.02	0.02 ± 0.02	0.02 ± 0.02	0.02 ± 0.01	0.02 ± 0.02
550	0.23 ± 0.08	0.11 ± 0.04	0.09 ± 0.03	0.09 ± 0.04	0.12 ± 0.02	0.14 ± 0.05
600	0.17 ± 0.08	0.18 ± 0.04	0.15 ± 0.02	0.14 ± 0.04	0.14 ± 0.06	0.16 ± 0.03
650	0.02 ± 0.04	0.12 ± 0.08	0.04 ± 0.03	0.02 ± 0.02	0.06 ± 0.08	0.02 ± 0.03
700	0.38 ± 0.15	0.43 ± 0.09	0.34 ± 0.04	0.31 ± 0.07	0.30 ± 0.10	0.37 ± 0.09
750	0.99 ± 0.01	0.75 ± 0.16	0.71 ± 0.12	0.73 ± 0.13	0.94 ± 0.09	0.83 ± 0.10
800	0.99 ± 0.01	0.90 ± 0.10	0.84 ± 0.07	0.88 ± 0.09	0.98 ± 0.02	0.94 ± 0.09
850	0.94 ± 0.04	0.94 ± 0.05	0.93 ± 0.05	0.93 ± 0.05	0.95 ± 0.04	0.95 ± 0.06
900	0.92 ± 0.04	0.98 ± 0.03	1.00 ± 0.00	1.00 ± 0.00	0.97 ± 0.05	0.99 ± 0.03
950	0.77 ± 0.02	0.90 ± 0.07	0.88 ± 0.05	0.88 ± 0.10	0.83 ± 0.07	0.89 ± 0.04
1000	0.71 ± 0.03	0.87 ± 0.08	0.83 ± 0.10	0.81 ± 0.12	0.78 ± 0.08	0.84 ± 0.05

In the next stage, an algorithm was developed to separate the fruit from the background. Reflectance values of the background were similar at wavelengths of 550 nm and 950 nm, while the fruits' reflectance was significantly different. Therefore, the background was eliminated from the images by subtracting the intensity values at these two wavelengths on a pixel-by-pixel basis and applying thresholding.

Within the framework of the present study, the applicability of a multispectral camera in distinguishing healthy from affected regions was investigated. The third stage involved analyzing the differences between healthy and defective areas on the segmented fruit. For each pixel, a correlation coefficient was calculated between its spectral signature and the reference spectrum of a healthy region in the 750–1000 nm range. Since suberinization exhibited less pronounced differences than other defects, an additional comparison was performed by calculating the correlation coefficient between each pixel's spectral characteristics and the reference spectrum for this defect. Next, segmentation into healthy and affected regions was carried out under the following conditions: for the first comparison, the correlation coefficient had to be below a threshold t_1, while for the second comparison, the correlation coefficient had to exceed a threshold t_2. Since the resulting defect mask contained misclassified pixels, we applied morphological processing. Morphological processing removed isolated pixels or single-pixel horizontal and vertical lines unless they were associated with areas larger than 10 pixels; horizontal and vertical lines longer than 3 pixels; objects smaller than 10 pixels; objects without areas 3 pixels thick in either direction; and closed areas.

2.4. Statistical Analysis

To determine the optimal threshold values, all data (764,091 healthy pixels and 914,592 affected pixels) were divided into reference (15%), training (70%), and test (15%) subsets. The proportions of the different classes were preserved across all subsets. The selection of thresholds t_1 and t_2 was performed based on the F1-score they achieved, with threshold values ranging from -1 to 1 in increments of 0.1. Model performance was evaluated using the following metrics: accuracy (ACC), precision (Pr), recall (Re), specificity (Sp), negative predictive value (NPV), false positive rate (FPR), false negative rate (FNR), and F1-score in arbitrary units.

Biochemical data were analyzed with the Microsoft Excel data analysis toolkit. For each parameter, the mean value and standard deviation were calculated. The significance of differences between groups was assessed using one-way analysis of variance (ANOVA). The difference with healthy samples was considered statistically significant at $p < 0.05$. Five biological replicates per defect type were involved in the analysis.

3. Results

Biochemical analysis showed that healthy fruits had the highest malic acid content (2.41 ± 0.15 mg/g), indicating they were not overripe. In contrast, all damaged fruits had significantly lower levels, ranging from 0.52 mg/g to 0.83 mg/g. The lowest levels were detected in fruits with gray mold (0.52 ± 0.03 mg/g, $p < 0.001$) and bruises (0.56 ± 0.04 mg/g, $p < 0.001$), confirming advanced physiological degradation.

Citric acid levels were generally high across all samples (11.40–13.33 mg/g), except for the fruits affected by gray mold, which contained only 0.10 ± 0.02 mg/g ($p < 0.001$). This significant decrease indicates that metabolic processes, particularly respiration, had nearly stopped. These fruits also showed the highest levels of succinic acid (0.23 ± 0.02 mg/g, $p < 0.001$), which is known to accumulate during storage and may signal cellular toxicity.

Total sugar (mono- and disaccharides) content was the highest in healthy fruits (219.50 ± 12.45 mg/g). Fruits affected by anthracnose had the lowest sugar content (78.20 ± 5.67 mg/g, $p < 0.001$), likely due to the pathogen's active consumption of carbohydrates. Samples with stink bug damage and suberinization had intermediate values (127.36 ± 9.45 and 128.37 ± 8.98 mg/g, respectively) ($p < 0.001$).

Samples with anthracnose, suberinization, and stink bug damage showed the highest total polyphenol concentrations (0.24 ± 0.02 mg/g and 0.23 ± 0.02 mg/g, $p < 0.01$), supporting the activation of defense mechanisms. A sharp decrease in polyphenols was observed in gray mold (0.05 ± 0.01 mg/g), indicating deep tissue degradation and suppression of secondary compound metabolism ($p < 0.01$).

The optimal thresholds were determined to be $t_1 = 0.6$ and $t_2 = 0.9$ (Figure 4). These thresholds were used to demonstrate the feasibility of the proposed approach (Figure 5).

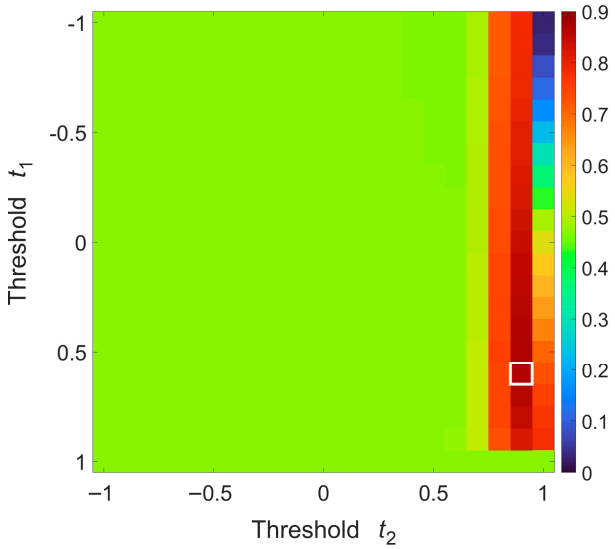


Figure 4. F1-score for different threshold combinations. The white square indicates the F1-score at the selected threshold values.

As shown in Figure 5, the algorithm can identify significant defects and small lesions that may expand over time, reducing fruit quality. The quantitative metrics of the algorithm's performance are shown in Table 2.

Table 2. Quantitative evaluation of the detection algorithm performance.

ACC	Pr	Re	Sp	NPV	FPR	FNR	F1-Score
0.94	0.90	0.89	0.96	0.96	0.04	0.12	0.90

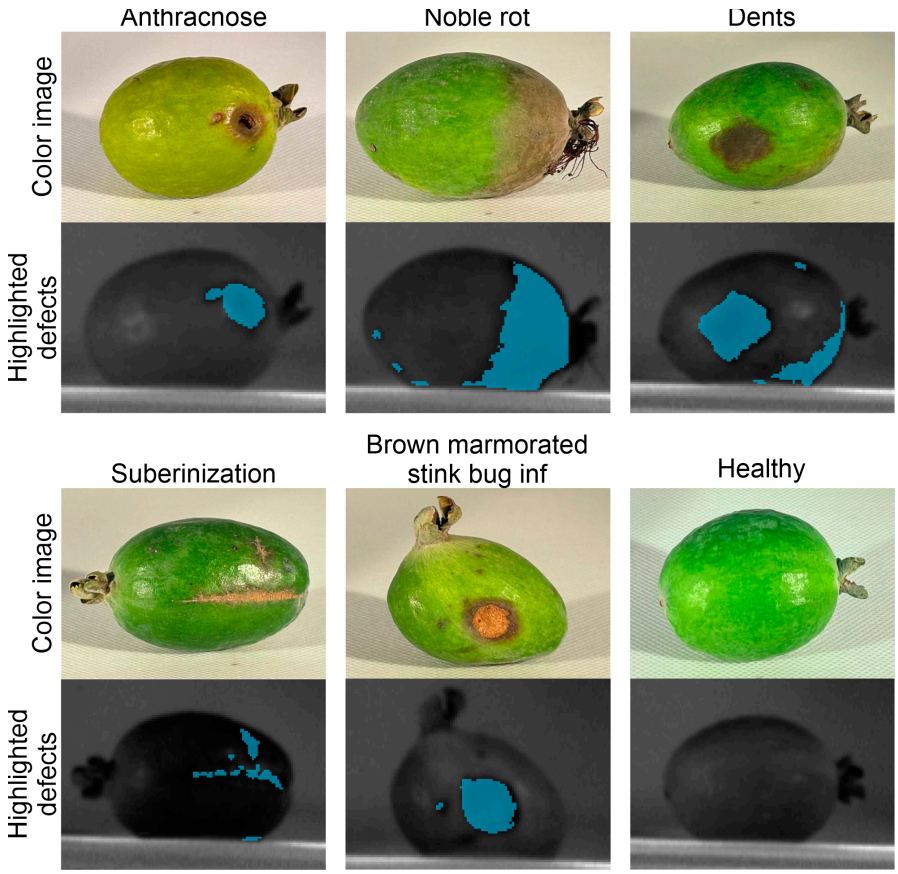


Figure 5. Defect segmentation.

Feijoa fruits with various types of damage pose a critical risk during storage [13] and must be removed from the commercial batch. Damaged fruits not only spoil themselves but also affect the quality of healthy ones by altering their biochemical composition and sensory properties. The proposed method advances a non-invasive multispectral imaging approach, making it a practical and reliable solution for early defect detection and quality assessment in research and industry. The automated detection algorithm effectively identifies different types of defect areas by analyzing multispectral data within the most relevant spectral channels.

4. Discussion

Feijoa fruits with various types of damage pose a significant risk during storage, necessitating their removal from the commercial batch [4]. Damaged fruits not only spoil themselves but also compromise the quality of healthy ones by altering their biochemical makeup and sensory properties. The proposed method introduces a non-invasive multispectral imaging approach, making it a practical and reliable solution for early defect detection and quality assessment in research and industry. The automated detection algorithm effectively identifies different defect types by analyzing multispectral data within the most relevant spectral channels.

A key advantage of the proposed approach is the use of a non-scanning multispectral system [17], which is optimal for high-throughput screening. These systems acquire spectral images simultaneously and reduce algorithmic complexity without compromising data collection or processing speed. Hyperspectral imaging offers an alternative approach for analyzing reflectance spectra, providing high spectral and spatial resolution. However, hyperspectral systems often require spectral and/or spatial scanning, leading to long data acquisition and processing times that limit real-time defect detection [18]. Tra-

ditional biochemical monitoring methods [19] are highly accurate but time-consuming and resource-intensive. Their limitations restrict their use in rapid plant disease diagnosis. The multispectral imaging approach overcomes these challenges and appears to be an optimal solution.

The proposed multispectral approach offers several key advantages. First, it significantly increases acquisition speed compared to hyperspectral systems, which typically capture full spectral image sets at about 1 Hz. In contrast, the spectral imaging method is mainly limited by the sensor's acquisition speed; currently, up to 20 Hz at full camera resolution is achievable. The data processing speed largely depends on the system's computational power. However, the proposed algorithm is not computationally intensive and allows segmentation of a spectral image set in roughly 1 s on a modest-performance computer (~0.5 TFLOPS). At the same time, this approach provides accuracy comparable to other multispectral systems and approaches some hyperspectral methods (~90–97%) [20–22]. Many studies have investigated the use of RGB imaging for fruit defect analysis; however, spectral imaging generally performs better, especially for early-stage detection [23,24]. The imaging process requires relatively low setup demands while offering high throughput and generally lower cost, which distinguishes the proposed approach from optical coherence tomography or fluorimetry systems [25,26].

Several studies have demonstrated that multispectral imaging is an effective tool for non-destructive defect detection in apples [27,28] and citrus fruits [29,30], enabling the identification of both external and internal damage by analyzing reflectance in specific spectral bands. A system that employs four broad spectral channels in the visible and near-infrared range has achieved real-time detection of citrus defects with over 95% accuracy [31]. A similar setup using channels at 450 nm, 500 nm, 750 nm, and 800 nm with respective bandwidths of 80 nm, 40 nm, 80 nm, and 50 nm, respectively, allowed the identification of defective bicolor apples with 90% accuracy [32]. A key limitation of other multispectral imaging systems is the limited number of spectral channels. In this study, we used a camera with changeable spectral filters. This flexibility is advantageous for manufacturers, as it supports a modular system design, even for specialized applications, ultimately reducing production costs. Moreover, a single device equipped with multiple filter arrays can be adapted to a wide range of tasks, making it particularly useful for research. For end users, the system offers compactness and lower cost than hyperspectral solutions. In addition to its flexible spectral channel configuration, the proposed camera offers advantages over other multispectral systems, including the absence of inter-channel crosstalk and precise synchronization between spectral images.

Despite its advantages, this approach has some limitations. Defects caused by suberization are not always reliably detected by correlation analysis alone, as their spectral response closely matches that of healthy tissue in certain wavelength ranges. Due to the fruit's curved surface, lighting across the image was uneven, leading to shadows near the edges. These shaded areas were sometimes misclassified as defects, as seen in the healthy fruit shown in Figure 4. This issue could be resolved at the image acquisition stage by optimizing the lighting setup [33] or at the image processing stage by normalizing surface brightness. Furthermore, the selection of optimal threshold values and the evaluation of the algorithm relied on manually annotated reference defect regions. Although this approach is not highly efficient, it is only required during the training phase and therefore does not affect the speed or reproducibility of subsequent routine assessments. Given that visual inspection remains the primary method for defect evaluation at present, full automation of this step cannot yet be considered a sufficiently reliable alternative [34]. Another limitation is the dataset's restricted scope, which includes only a single cultivar and a specific imaging setup. Further studies are required to ensure generalization across different cultivars,

storage conditions, and imaging scenarios, such as when fruits are arranged in multiple layers. In the present study, we employed a classical computer vision algorithm without deep learning. As numerous studies report successful applications of both approaches to fruit defect detection, a comparative evaluation of their applicability to data from the proposed camera and to feijoa analysis should be conducted. [14,35,36].

A particularly promising application of this method is the automated removal of substandard feijoa fruits. By integrating multispectral imaging with machine learning algorithms, it is possible to develop high-throughput quality control systems that operate in real-time mode without human oversight [37]. This technology can significantly enhance the efficiency of sorting lines and mobile units during the harvest, ensuring optimal organization and productivity [22]. It also offers valuable capabilities for warehouse monitoring, detecting early signs of spoilage or hidden defects that could affect long-term storage quality. Additionally, the method may support experimental testing of storage extension technologies, enabling rapid, non-invasive assessment of fruit conditions throughout the supply chain. A promising direction for future work is the incorporation of three-dimensional surface profile assessment of the fruit [38].

5. Conclusions

In this study, we analyzed defects on *Feijoa sellowiana* fruits using a multispectral imaging system. The study identified the most informative spectral ranges centered at 550 nm, 750 nm, 950 nm, and 1000 nm wavelengths. A data processing algorithm was developed to detect five types of feijoa defects: bruises, anthracnose, stink bug damage, tissue suberization, and gray mold. The findings can help develop methods for automated defect detection in feijoa fruits through multispectral imaging and machine learning. Incorporating this approach as a preliminary diagnostic step alongside traditional methods can improve the efficiency and speed of phytopathology detection. It also helps prevent the spread of defective fruits within the batch, reducing losses and ensuring production profitability by cutting down the time needed for laboratory verification.

Author Contributions: Conceptualization, A.M.; methodology, A.M. and A.G.; software, S.B.; validation, formal analysis, A.Z., S.B., N.P. and V.K.; investigation, A.Z., N.P. and V.K.; resources, A.M.; data curation, A.Z. and S.B.; writing—original draft preparation, A.Z.; writing—review and editing, A.Z., S.B., A.G., A.M., N.P. and V.K.; visualization, A.Z. and S.B.; supervision, A.Z., A.G. and A.M.; project administration A.G. and A.M.; funding acquisition, A.M. All authors have read and agreed to the published version of the manuscript.

Funding: This study is supported by the Russian Science Foundation (project 25-16-00121). The experimental protocol, sample preparation and laboratory tests were performed within the Federal State Task of the Subtropical Scientific Centre of the Russian Academy of Sciences (project FGRW-2025-0005, registration number 12507180812-9).

Data Availability Statement: The data generated and analyzed during this study are available from the corresponding author upon reasonable request.

Acknowledgments: This work was performed using the equipment of the Center for Collective Use of STC UI RAS [https://ckp.ntcup.ru/en/].

Conflicts of Interest: The authors declare no conflicts of interest.

References

1. Omarov, M.D.; Omarova, Z.M.; Karpun, N.N. *Feijoa Cultivation in the Humid Subtropics of Russia: A Monograph*; Federal Research Center "Subtropical Scientific Center of the Russian Academy of Sciences": Sochi, Russia, 2022.
2. Ramírez, F.; Kallarackal, J. Feijoa [*Acca sellowiana* (O. Berg) Burret] Pollination: A Review. *Sci. Hortic.* **2017**, *226*, 333–341. [CrossRef]

3. El-Gholl, N.E.; Alfieri, S.A., Jr.; Schubert, T.S.; Schoulties, C.L. *Pseudocercospora feijoae* sp. Nov. Causing a Leaf Spot Disease on *Feijoa sellowiana* in Florida. *Mycologia* **1988**, *80*, 769–775. [CrossRef]
4. Klein, J.D.; Thorp, T.G. Feijoas: Post-Harvest Handling and Storage of Fruit. *N. Z. J. Exp. Agric.* **1987**, *15*, 217–221. [CrossRef]
5. Bentancourt, C.M.; Scatoni, I.B. *Guía de Insectos y Ácaros de Importancia Agrícola y Forestal en el Uruguay*, 3rd ed.; Facultad de Agronomía de la Universidad de la República: Montevideo, Uruguay, 2010.
6. Phan, A.D.T.; Chaliha, M.; Sultanbawa, Y.; Netzel, M.E. Nutritional Characteristics and Antimicrobial Activity of Australian Grown Feijoa (*Acca sellowiana*). *Foods* **2019**, *8*, 376. [CrossRef]
7. Soltani Firouz, M.; Sardari, H. Defect Detection in Fruit and Vegetables by Using Machine Vision Systems and Image Processing. *Food Eng. Rev.* **2022**, *14*, 353–379. [CrossRef]
8. Smeriglio, A.; Denaro, M.; De Francesco, C.; Cornara, L.; Barreca, D.; Bellocco, E.; Ginestra, G.; Mandalari, G.; Trombetta, D. Feijoa Fruit Peel: Micro-Morphological Features, Evaluation of Phytochemical Profile, and Biological Properties of Its Essential Oil. *Antioxidants* **2019**, *8*, 320. [CrossRef]
9. Rojas Santelices, I.; Cano, S.; Moreira, F.; Peña Fritz, Á. Artificial Vision Systems for Fruit Inspection and Classification: Systematic Literature Review. *Sensors* **2025**, *25*, 1524. [CrossRef] [PubMed]
10. Li, J.B.; Huang, W.Q.; Zhao, C.J. Machine Vision Technology for Detecting the External Defects of Fruits—A Review. *Imaging Sci. J.* **2015**, *63*, 241–251. [CrossRef]
11. Saleah, S.A.; Kim, S.; Luna, J.A.; Wijesinghe, R.E.; Seong, D.; Han, S.; Kim, J.; Jeon, M. Optical Coherence Tomography as a Non-Invasive Tool for Plant Material Characterization in Agriculture: A Review. *Sensors* **2023**, *24*, 219. [CrossRef] [PubMed]
12. Huang, Z.; Saito, Y.; Gao, T.; Al Riza, D.F.; Lu, R.; Cen, H.; Kondo, N.; Omwange, K.A. A Review of Fluorescence Imaging System Supported by Excitation-Emission Matrix for Fruit and Vegetable Quality Estimation. *Food Control* **2025**, *169*, 111040. [CrossRef]
13. Garini, Y.; Young, I.T.; McNamara, G. Spectral Imaging: Principles and Applications. *Cytom. Part A* **2006**, *69*, 735–747. [CrossRef]
14. Tao, T. Multispectral Method for Apple Defect Detection Using Hyperspectral Imaging System. Doctoral Dissertation, University of Maryland, College Park, MD, USA, 2011.
15. Batshev, V.I.; Batshev, V.I.; Krioukov, A.V.; Krioukov, A.V.; Krioukov, A.V.; Machikhin, A.S.; Machikhin, A.S.; Zolotukhina, A.A.; Zolotukhina, A.A. Multispectral Video Camera Optical System. *J. Opt. Technol.* **2023**, *90*, 706–712. [CrossRef]
16. Pu, R. *Hyperspectral Remote Sensing: Fundamentals and Practices*; CRC Press: Boca Raton, FL, USA, 2017; pp. 1–466. [CrossRef]
17. Hagen, N.A.; Kudenov, M.W. Review of Snapshot Spectral Imaging Technologies. *Opt. Eng.* **2013**, *52*, 090901. [CrossRef]
18. Bhargava, A.; Sachdeva, A.; Sharma, K.; Alsharif, M.H.; Uthansakul, P.; Uthansakul, M. Hyperspectral Imaging and Its Applications: A Review. *Heliyon* **2024**, *10*, e33208. [CrossRef]
19. Khakimov, A.; Salakhutdinov, I.; Omolikov, A.; Utaganov, S. Traditional and Current-Prospective Methods of Agricultural Plant Diseases Detection: A Review. In *IOP Conference Series: Earth and Environmental Science*; IOP Publishing: Bristol, UK, 2022; Volume 951, p. 012002. [CrossRef]
20. Zhang, H.; Zhang, S.; Dong, W.; Luo, W.; Huang, Y.; Zhan, B.; Liu, X. Detection of Common Defects on Mandarins by Using Visible and near Infrared Hyperspectral Imaging. *Infrared Phys. Technol.* **2020**, *108*, 103341. [CrossRef]
21. Zhang, L.; Nie, P.; Zhang, S.; Zhang, L.; Sun, T. Research on Defect Detection in Kubo Peach Based on Hyperspectral Imaging Technology Combined with CARS-MIV-GA-SVM Method. *Foods* **2023**, *12*, 3593. [CrossRef] [PubMed]
22. Khort, D.O.; Kutyrev, A.; Smirnov, I.; Andriyanov, N.; Filippov, R.; Chilikin, A.; Astashev, M.E.; Molkova, E.A.; Sarimov, R.M.; Matveeva, T.A.; et al. Enhancing Sustainable Automated Fruit Sorting: Hyperspectral Analysis and Machine Learning Algorithms. *Sustainability* **2024**, *16*, 10084. [CrossRef]
23. Rouš, R.; Peller, J.; Polder, G.; Hageraats, S.; Ruigrok, T.; Blok, P.M. Apple Scab Detection in Orchards Using Deep Learning on Colour and Multispectral Images. *arXiv* **2023**, arXiv:2302.08818. [CrossRef]
24. Batashova, S.S.; Zolotukhina, A.A.; Guryleva, A.V.; Platonova, N.B.; Kunina, V.A. Method for Automated Evaluation of the Efficiency of Fruit Preservatives Using an Acousto-Optical Video Spectrometer. *Opt. J.* **2024**, *91*, 452–458. [CrossRef]
25. Mariani, S.; Dhanushka Karunanayaka, A.; Shantha Kahatapitiya, N.; Damith, N.; Kim, J.; Jeon, M.; Silva, B.N.; Eranga Wijesinghe, R.; Wijenayake, U. Non-Invasive Disease Stage Classification of Bitter Rot in Fruits Using Optical Coherence Tomography and Intensity-Based Image Analysis. *Eng. Proc.* **2025**, *118*, 95. [CrossRef]
26. Momin, A.; Kondo, N.; Al Riza, D.F.; Ogawa, Y.; Obenland, D. A Methodological Review of Fluorescence Imaging for Quality Assessment of Agricultural Products. *Agriculture* **2023**, *13*, 1433. [CrossRef]
27. Lee, H.; Yang, C.-C.; Kim, M.S.; Lim, J.; Cho, B.-K.; Lefcourt, A.; Chao, K.; Everard, C.D. A Simple Multispectral Imaging Algorithm for Detection of Defects on Red Delicious Apples. *J. Biosyst. Eng.* **2014**, *39*, 142–149. [CrossRef]
28. Alam, M.N.; Pineda, I.; Lim, J.G.; Gwun, O. Apple Defects Detection Using Principal Component Features of Multispectral Reflectance Imaging. *Sci. Adv. Mater.* **2018**, *10*, 1051–1062. [CrossRef]
29. Aleixos, N.; Blasco, J.; Navarrón, F.; Moltó, E. Multispectral Inspection of Citrus in Real-Time Using Machine Vision and Digital Signal Processors. *Comput. Electron. Agric.* **2002**, *33*, 121–137. [CrossRef]

30. Bulanon, D.M.; Burks, T.F.; Alchanatis, V. A Multispectral Imaging Analysis for Enhancing Citrus Fruit Detection. *Environ. Control. Biol.* **2010**, *48*, 81–91. [CrossRef]
31. Abdelsalam, A.M.; Sayed, M.S. Real-Time Defects Detection System for Orange Citrus Fruits Using Multi-Spectral Imaging. In Proceedings of the 2016 IEEE 59th International Midwest Symposium on Circuits and Systems (MWSCAS), Abu Dhabi, United Arab Emirates, 16–19 October 2016. [CrossRef]
32. Kleynen, O.; Leemans, V.; Destain, M.F. Development of a Multi-Spectral Vision System for the Detection of Defects on Apples. *J. Food Eng.* **2005**, *69*, 41–49. [CrossRef]
33. Jong, L.J.S.; Post, A.L.; Geldof, F.; Dashtbozorg, B.; Ruers, T.J.M.; Sterenborg, H.J.C.M. Separating Surface Reflectance from Volume Reflectance in Medical Hyperspectral Imaging. *Diagnostics* **2024**, *14*, 1812. [CrossRef] [PubMed]
34. Wang, B.; Yang, H.; Zhang, S.; Li, L. Detection of Defective Features in Cerasus Humilis Fruit Based on Hyperspectral Imaging Technology. *Appl. Sci.* **2023**, *13*, 3279. [CrossRef]
35. Zhang, B.; Liu, L.; Gu, B.; Zhou, J.; Huang, J.; Tian, G. From Hyperspectral Imaging to Multispectral Imaging: Portability and Stability of HIS-MIS Algorithms for Common Defect Detection. *Postharvest Biol. Technol.* **2018**, *137*, 95–105. [CrossRef]
36. Ryu, J.; Kim, S.Y.; Lee, C.H.; Kim, G.; Jang, H.; Kim, T.; Hong, S.J.; Kim, G.H.; Kim, G. Enhancement of Apple Defect Identification with Semantic Segmentation and Label-Efficient Data Generation. *Eng. Appl. Artif. Intell.* **2026**, *163*, 112679. [CrossRef]
37. Deng, D.; Liu, Z.; Lv, P.; Sheng, M.; Zhang, H.; Yang, R.; Shi, T. Defect Detection in Food Using Multispectral and High-Definition Imaging Combined with a Newly Developed Deep Learning Model. *Processes* **2023**, *11*, 3295. [CrossRef]
38. Naqvi, L.H.; Balasubramaniam, B.; Li, J.; Liu, L.; Li, B. Four-Dimensional Hyperspectral Imaging for Fruit and Vegetable Grading. *Agriculture* **2025**, *15*, 1702. [CrossRef]

Disclaimer/Publisher's Note: The statements, opinions and data contained in all publications are solely those of the individual author(s) and contributor(s) and not of MDPI and/or the editor(s). MDPI and/or the editor(s) disclaim responsibility for any injury to people or property resulting from any ideas, methods, instructions or products referred to in the content.